Purdue University
Purdue e-Pubs

Birck and NCN Publications | Birck Nanotechnology Center

3-11-2009

A nanofluidic channel with embedded transverse nanoelectrodes

T Maleki
Purdue University - Main Campus

Saeed Mohammadi
School of Electrical and Computer Engineering, Purdue University, saeedm@purdue.edu

Babak Ziaie
Birck Nanotechnology Center, Purdue University, bziaie@purdue.edu

Follow this and additional works at: https://docs.lib.purdue.edu/nanopub

 Part of the Nanoscience and Nanotechnology Commons

Maleki, T; Mohammadi, Saeed; and Ziaie, Babak, "A nanofluidic channel with embedded transverse nanoelectrodes" (2009). *Birck and NCN Publications.* Paper 372.
https://docs.lib.purdue.edu/nanopub/372

This document has been made available through Purdue e-Pubs, a service of the Purdue University Libraries. Please contact epubs@purdue.edu for additional information.

Nanotechnology **20** (2009) 105302 (6pp) doi:10.1088/0957-4484/20/10/105302

A nanofluidic channel with embedded transverse nanoelectrodes

T Maleki[1,2], **S Mohammadi**[1,2] **and B Ziaie**[1,2,3,4]

[1] School of Electrical and Computer Engineering, Purdue University, West Lafayette, IN, USA
[2] Birck Nanotechnology Center, Purdue University, West Lafayette, IN, USA
[3] Weldon School of Biomedical Engineering, Purdue University, West Lafayette, IN, USA

E-mail: bziaie@purdue.edu

Received 17 November 2008, in final form 15 January 2009
Published 16 February 2009
Online at stacks.iop.org/Nano/20/105302

Abstract

In this paper, we demonstrate fabrication and characterization of a nanofluidic channel with embedded transverse nanoelectrodes using a combination of conventional photolithography and focused ion beam technologies. Glass-capped silicon dioxide nanochannels having 20 nm depth, 50 nm width, and 2 μm length with embedded platinum nanoelectrodes were fabricated. Channel patency was verified through measurements of the resistivity in phosphate buffered saline and electrostatic action on charged fluorescent nanospheres. Platinum nanoelectrode functionality was also tested using transverse resistance measurements in nanochannels filled with air, deionized water, and saline solution.

(Some figures in this article are in colour only in the electronic version)

1. Introduction

Fabrication of nanochannels is attracting considerable interest due to its broad applications in nanobiotechnology (e.g., biomolecular sensing and single DNA manipulation) [1–5] and its utility in fundamental studies related to the physical effects governing nano-confined liquids and gases [6–9]. While fabrication of inorganic nanopores, which is mostly driven by their application in DNA sequencing and molecular sensing [10–14], has become relatively mature; nanochannel fabrication and its subsequent filling have proven to be more challenging tasks. As compared to nanopores, nanochannels offer distinct advantages in allowing a slower translocation and multiple sensing spots along the channel both of which improves the read-out resolution [15]. Literature concerning the methods of fabrication for nanochannels is rather extensive, covering technologies such as bulk micromachining [16, 17], surface micromachining [18], thermal oxidation with anodic bonding [19], thermal oxidation with chemical–mechanical polishing [20], nano-imprint lithography with subsequent dielectric sputtering [21], and focused ion beam (FIB) milling of solid surfaces [22] to name a few.

Beyond the ability to fabricate a nanochannel, two other highly desirable characteristics are optical and electrical

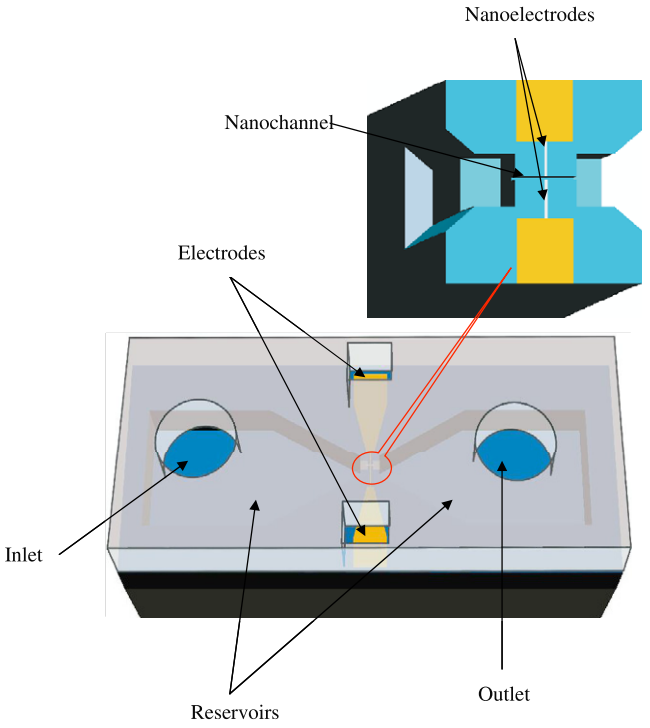

Figure 1. 3D schematic of the nanoelectrode embedded nanochannel showing reservoirs, electrodes, and inlet/outlet. The nanochannel and nanoelectrodes are also shown.

[4] Author to whom any correspondence should be addressed.

 © 2009 IOP Publishing Ltd Printed in the UK

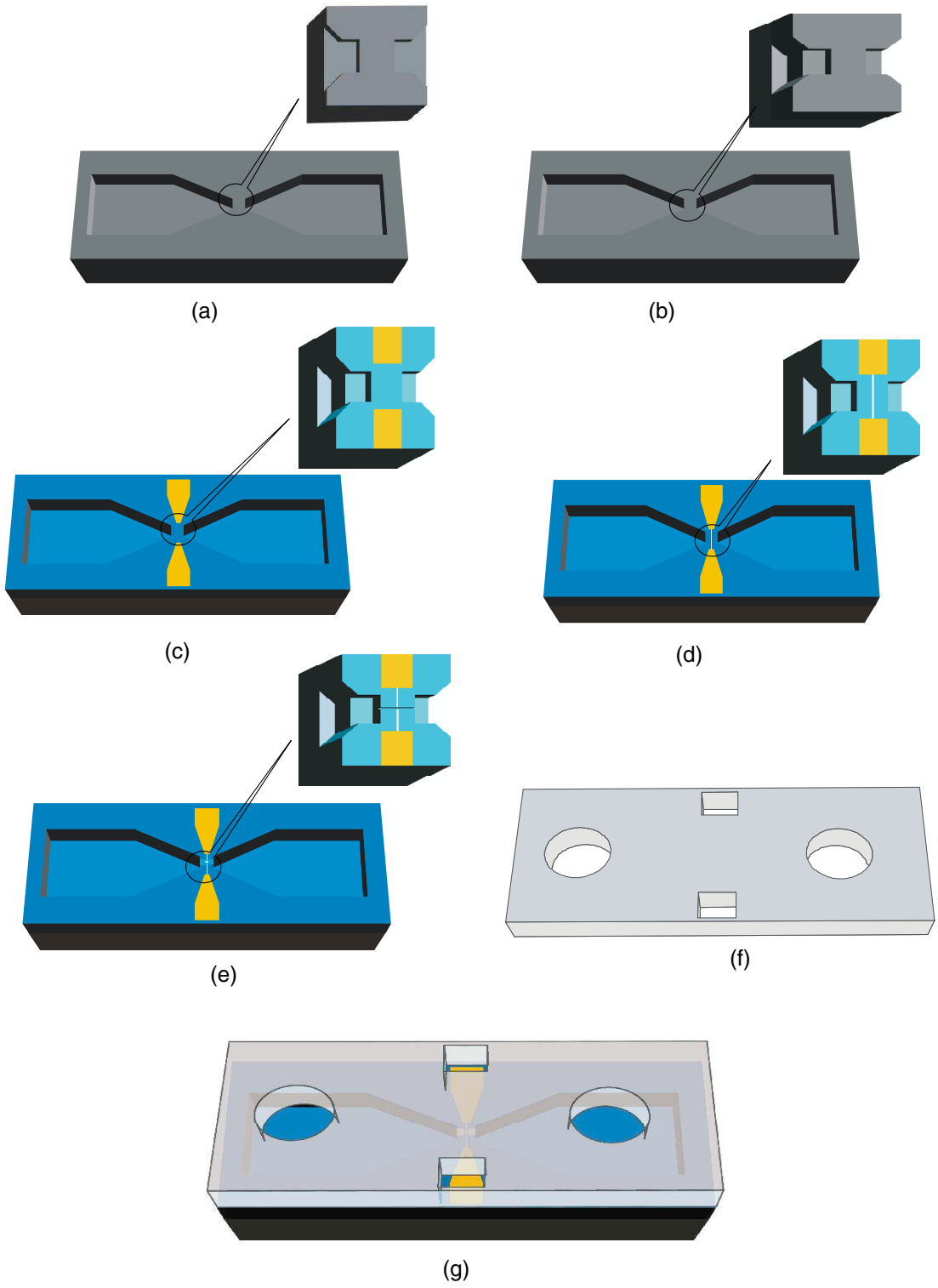

Figure 2. Nanoelectrode embedded nanochannel fabrication process including two steps of DRIE (a), (b), modified lift-off (c), FIB-assisted nanoelectrode–nanochannel fabrication (d), (e), and anodic bonding (g).

accessibility. The former requires that the nanochannel be transparent to the light at least in one direction, thus allowing real time microscopic examination; while the latter provides electrical access for measurement and flow control via Debye length modulation [23]. The transparency requirement is easier to achieve by using a suitable substrate (glass or quartz), however, implementing nano-scale electrical contacts inside the nanochannel is not trivial and to our knowledge has not been demonstrated.

In this paper, we present the fabrication of a nanofluidic channel with embedded transverse nanoelectrodes using a combination of conventional photolithography and focused ion beam (FIB) technologies. The fabricated channels completely reside inside silicon dioxide which is one of the most studied

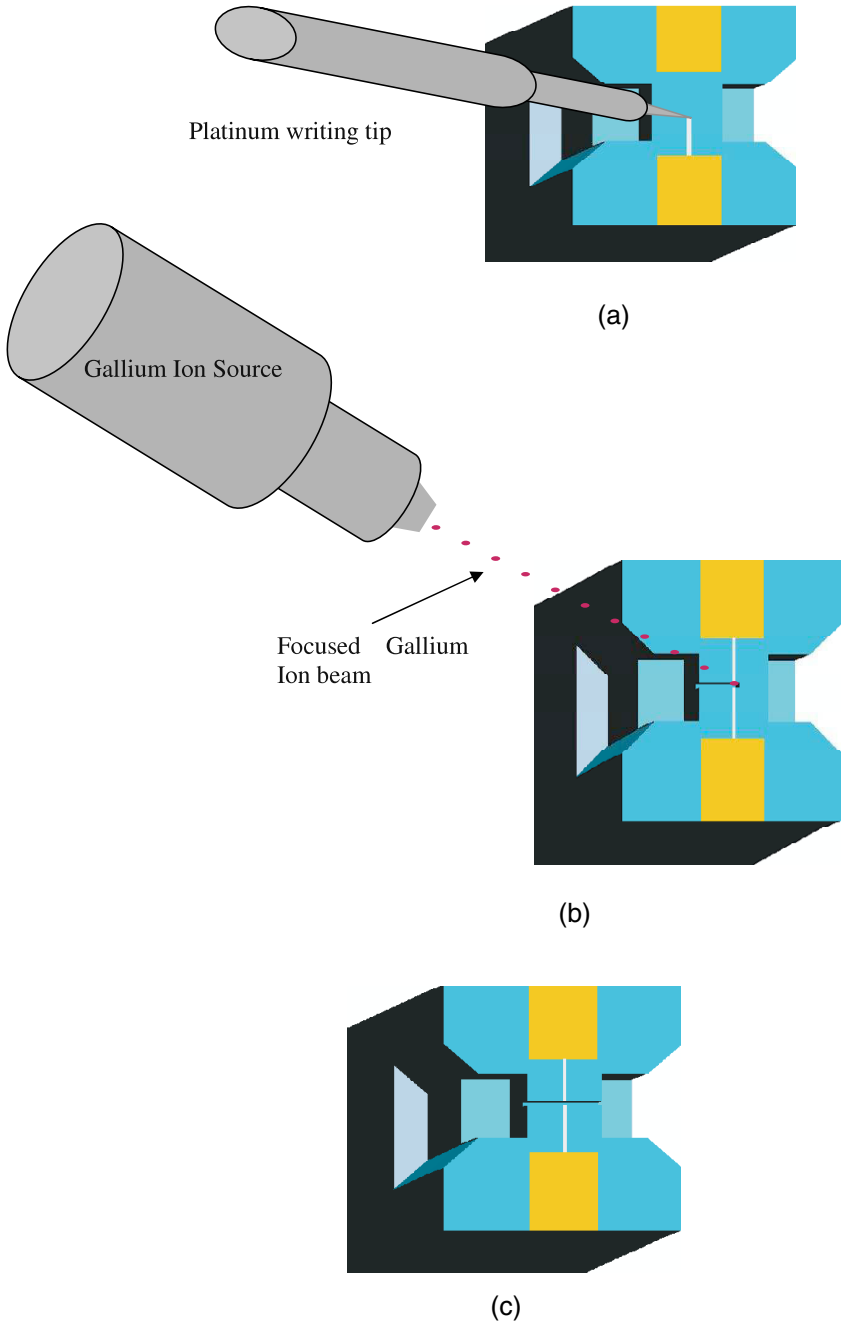

Figure 3. FIB-assisted nanoelectrode–nanochannel fabrication process.

and characterized surfaces used for biological applications. Optically transparent borosilicate glass was used as the top coverage, providing a window for real time fluorescent microscopy. Parts of the electrodes in contact with liquid were made of platinum for electrochemical compatibility.

2. Fabrication process

Figure 1 illustrates the 3D schematic of the device. It consists of an inlet and outlet for sample introduction, micro-scale leading reservoirs, a nanochannel, electrical access holes, micro-scale leading electrodes, and two nanoelectrodes. The fabrication process for the nanofluidic channel with embedded transverse nanoelectrodes is depicted in figure 2. Micro-scale leading reservoirs were fabricated using a two-step dry etch process (deep reactive ion etching, DRIE) in a high resistivity silicon wafer to create: (1) larger and deeper (150 μm in depth) reservoirs to accommodate the inlet and outlet tubing junctions, and (2) shallower microchannels (1 μm in depth) connected to the deep reservoirs. The shallower regions were required for subsequent microelectrode fabrication step in which a fine alignment was needed. In order to accomplish the required lithography, a deep microchannel close to the microelectrodes had to be avoided since it prevents adequate photoresist step coverage. The two-step microreservoir fabrication process was done by etching the shallower microchannel first using DRIE

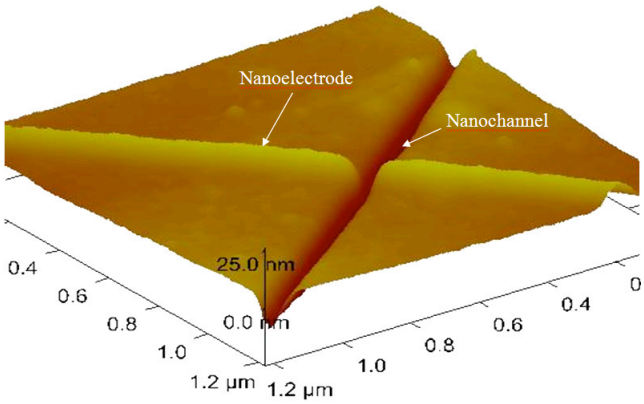

Figure 4. AFM image of the nanoelectrode–nanochannel clearly showing no blockage in the nanochannel at the nanoelectrode location.

followed (figure 2(a)) by covering the central etched area by a photoresist droplet and continuing the DRIE until 150 μm deeper reservoirs were fabricated (figure 2(b)).

Following the fabrication of the micro-reservoirs a 700 nm thick thermal oxide was grown on the surface. This step was followed by deposition and lift-off of 10 nm Cr/100 nm Au layer for the microelectrodes, figure 2(c). A modified lift-off process was employed to achieve a planar surface after metallization. This is crucial for the quality of subsequent anodic bonding process since any step height greater that 50 nm creates unbounded areas [24]. The lift-off process was modified by etching a 100 nm recess in the top oxide layer (Plasmatech RIE) after photoresist patterning and prior to metallization. This modification in lift-off process ensures a step height of only ∼10 nm.

Nanochannel and nanoelectrodes were fabricated using high resolution FIB (FEI Nova 200©) as depicted in figures 2(d) and (e). First, FIB-assisted deposition was used to create a 40 nm wide and 10 nm thick platinum line connecting the two Cr/Au microelectrodes, figure 3(a). Then, FIB was used to cut a 50 nm wide and 20 nm deep nanochannel in perpendicular direction, figures 3(b) and (c). FIB etches metals much faster than silicon dioxide, thus removing platinum and its underlying oxide in one single pass. Figure 4 shows an atomic force microscope image of the fabricated nanochannel (50 nm wide and 20 nm deep) and nanoelectrodes.

The top capping glass layer was prepared by drilling four 3 mm diameter holes in a Corning 7740 glass wafer using fine diamond coated drill bit. Two of these holes serve as inlet and outlet liquid access ports while the other two provide electrical access for the nanoelectrodes, figure 2(f). The glass wafer was then bonded to the prepared silicon substrate using high strength anodic bonding, figure 2(g) [25]. Oxygen plasma surface activation was used before bonding to facilitate the wetting of the nanochannels. Figures 5(a) shows the SEM micrograph of the nanoelectrodes and nanochannel before anodic bonding while figure 5(b) shows optical photograph of the completely fabricated micro-device.

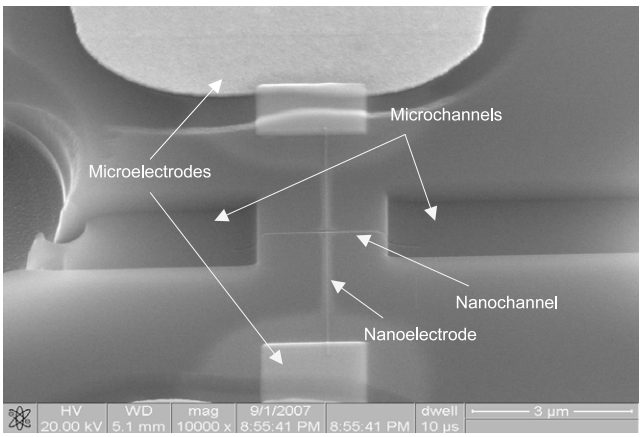

(a)

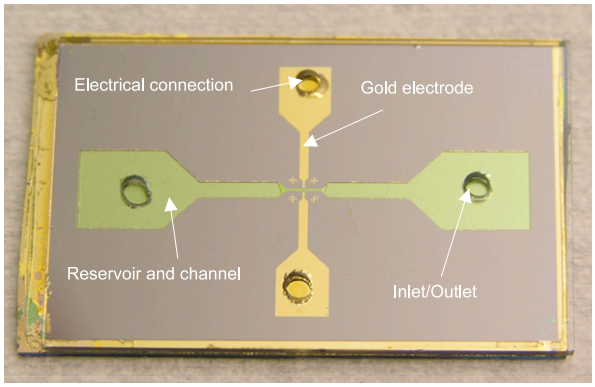

(b)

Figure 5. (a) Nanochannel–nanoelectrode SEM image before covering with glass, (b) optical photograph of the completed device.

3. Experimental results and discussion

Nanochannels were filled through the sequential steps of soaking in acetone, methanol, isopropanol alcohol (IPA) and DI water in a vacuum chamber (each soaking step was 30 min long). These steps are critical and are based on the fact that acetone wets the nanochannels much faster than DI water [26, 27]. It is however difficult to directly replace acetone with DI water due to their mutual immiscibility. Flushing the nanochannel with methanol and IPA prior to DI water solves the above mentioned problem. Following the wetting steps, inlet/outlet tubings were connected to the device and DI water was pumped through. This was done using two syringe pumps, one connected to the inlet and pushing the liquid while the second one sucking the water out through the outlet creating a high pressure gradient across the channel.

In order to verify the nanochannel functionality, we performed resistivity measurements by placing DI water at outlet of the channel and pumping 0.1 M phosphate buffered saline (PBS) from the inlet for two days (in this case the second outlet pump was not present and the outlet tubing was simply inserted into DI water). Figure 6 shows the measured resistivity of DI water at 1 kHz versus time. As can be seen, DI water resistivity drops as more PBS is pumped through the channel, thus verifying the nanochannel patency. We also

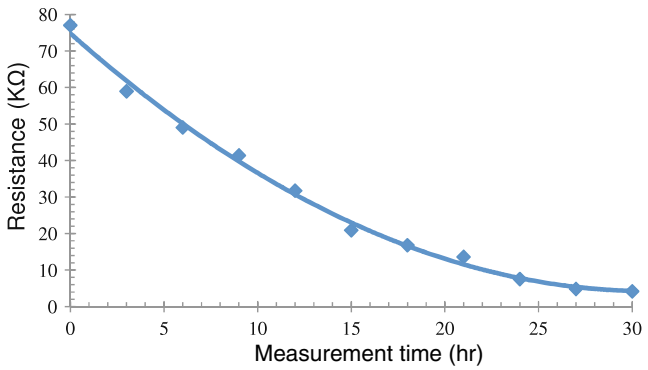

Figure 6. Measured resistivity of DI water versus time at 1 kHz as more PBS is introduced into the solution.

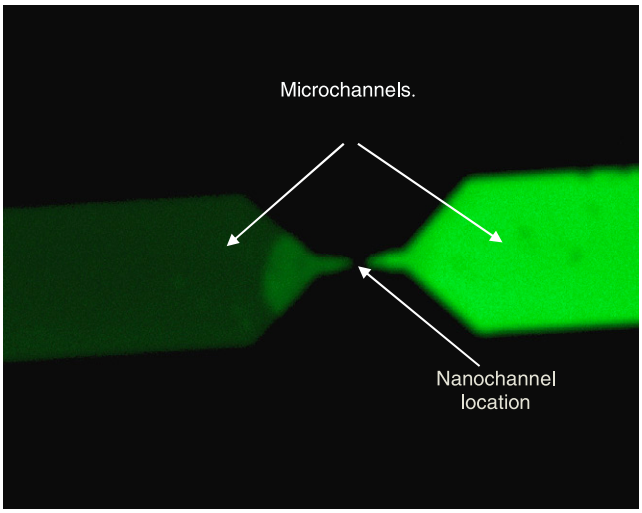

Figure 7. Fluorescent image of a nanochannel with fluorescence particles introduced at the inlet (right) and elecrophoretically migrated to the outlet (left).

electrophoretically pumped negatively charged FluoSpheres® carboxylate-modified nanospheres (20 nm nominal diameter, Invitrogen) through the nanochannel. To conduct this test, the nanochannel as well as the inlet and the outlet chambers were filled by 0.1 M PBS and FluoSpheres® was introduced into the grounded inlet while the outlet was connected to a positive voltage (10 V) thus forcing the negatively charged particles towards the outlet. Figure 7 shows a fluorescence image of the device clearly showing the movement of the fluorescence particles from the inlet (bright side) to the outlet thorough the nanochannel.

Finally, in order to test the functionality of the nanoelectrodes, we introduced PBS solutions of various concentrations and measured their resistivity. The resistance measurements were carried out while the channel was dry, wetted by DI water, and filled by different concentrations of PBS solution. As can been seen in figure 8, at dry state the resistance was very high (5×10^7 Ω), with DI water it dropped to 5×10^4 Ω, and thereafter decreased uniformly as more concentrated PBS solutions were introduced, clearly demonstrating the functionality of the nanoelectrodes,

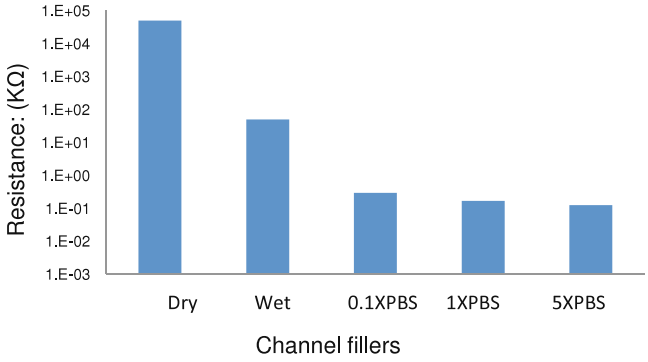

Figure 8. Transverse conductivity measurements using nanoelectrodes in a nanochannel (dry state, with DI water, and with PBS of different concentrations).

4. Summary

In this paper, we demonstrated the fabrication and characterization of a nanofluidic channel with embedded transverse nanoelectrodes for the first time. Fabrication process is simple and repeatable relying on conventional photolithography and FIB-assisted nanofabrication (deposition and etching). Nanochannels as small as 20 nm deep and 50 nm wide were successfully fabricated and characterized using resistivity measurements and fluorescence microscopy. The PBS-filled nanochannel transverse resistance between the nanoelectrodes was also measured in order to verify the nanoelectrode functionality.

Acknowledgments

The authors would like to thank Dr Demir Akin for his assistance in testing and fluorescence microscopy and Mr Dmitri Zakharov for his help in FIB. We would also like to thank the staff at the Purdue University Birck Nanotechnology Center for their assistance.

References

[1] Stern M B, Geis M W and Curtin J E 1997 Nanochannel fabrication for chemical sensors *J. Vac. Sci. Technol.* B **15** 2887–91
[2] Gawad S, Schild L and Renaud Ph 2001 Micromachined impedance spectroscopy flow cytometer for cell analysis and particle sizing *Lab Chip* **1** 76–82
[3] Stein D, Van der Heyden F H J, Koopmans W J A and Dekker C 2006 Pressure-driven transport of confined DNA polymers in fluidic channels *Proc. Natl Acad. Sci.* **103** 15853–8
[4] Reccius C H, Stavis S M, Mannion J T, Walker L P and Craighead H G 2008 Conformation, lenght, and speed measurement of electodynamically stretched DNA in nanochannels *Biophys. J.* **85** 273–86
[5] Reisner W, Morton K J, Reihn R, Wang Y M, Yu Z, Rosen M, Strum J C, Chou S Y, Frey E and Austin R H 2005 Statics and dynamics of single DNA molecules confined in nanochannels *Phys. Rev. Lett.* **94** 196101
[6] Pennathur S and Santiago J G 2005 Electrokinetic transport in nanochannels. 2. Experiments *Anal. Chem.* **77** 6782–9

[7] Qiao R and Aluru N R 2004 Charge inversion and flow reversal in a nanochannel electrosmotic flow *Phys. Rev. Lett.* **92** 198301
[8] Lu H, Li J, Gong X, Wan R, Zeng L and Fang H 2008 Water permeation and wavelike density distribution inside narrow channels *Phys. Rev.* B **77** 174115
[9] Jung Y 2007 Velocity inversion in nanochannel flow *Phys. Rev.* E **75** 051203
[10] Zwolak M and Ventra M D 2008 Physical approaches to DNA sequencing and detection *Rev. Mod. Phys.* **80** 141–65
[11] Healy K 2007 Nanopore-based single-molecule DNA analysis *Nanomedicine* **2** 459–81
[12] Aksimentiev A, Heng J B and Timp G 2004 Microscopic kinetics of DNA translocation through synthetic nanopores *Biophys. J.* **87** 2086–97
[13] Tas N R, Berenschot J W, Mela P, Jansen H V, Elwenspoek M and van den Berg A 2002 Functionalized nanopore-embedded electrodes for rapid DNA sequencing *Nano Lett.* **2** 1031–2
[14] Heng J B, Aksimentiev A, Ho C, Marks P, Grinkova Y V, Sligar S, Schulten K and Timp G 2006 The electromechanics of DNA in a synthetic nanopore *Biophys. J.* **90** 1098–106
[15] Tabard-Cossa V, Trivedi D, Wiggin M, Jetha N N and Marziali A 2007 Noise analysis and reduction in solid-state nanopores *Nanotechnology* **18** 305505
[16] Haneveld J, Jansen H, Berenschot E, Tas N and Elwenspoek M 2003 Wet anisotropic etching for fluidic 1D nanochannels *J. Micromech. Microeng.* **13** S62–6
[17] Mao P and Han J 2005 Fabrication and characterization of 20 nm planar nanofluidic channels by glass–glass and glass–silicon bonding *Lab Chip* **5** 837–44
[18] Tas N R, Berenschot J W, Mela P, Jensen H V, Elwenspoek M and van der Berg A 2002 2D-confined nanochannels fabricated by conventional micromachining *Nano Lett.* **2** 1031–2
[19] Wu C, Jin Z, Wang H, Ma H and Wang Y 2007 Design and fabrication of a nanofluidic channel by selective thermal oxidation and etching back of silicon dioxide made on a silicon substrate *J. Micromech. Microeng.* **17** 2393–7
[20] Lee C, Yang E H, Myung N V and George T 2003 A nanochannel fabrication technology without nanolithography *Nano Lett.* **3** 1339–40
[21] Cao H, Yu Z, Wang J, Tegenfelt J O, Austin R H, Wu W and Chou S Y 2002 Fabrication of 10 nm enclosed nanofluidic channel *Appl. Phys. Lett.* **81** 174–6
[22] Alarie J P, Hmelo A B, Jacobson S C, Baddorf A P, Feldman L and Ramsey J M 2003 *Fabrication and Evaluation of 2D Confined Nanochannels in Micro Total Analysis Systems* vol 1 ed M A Northrup, K F Jensen and D J Harrison (Cleveland Heights, OH: Transducers Research Foundation) pp 9–12
[23] Karnik R, Fan R, Yue M, Li D, Yang P and Majumdar A 2005 Electrostatic control of ions and molecules in nanofluidic transistors *Nano Lett.* **5** 943–8
[24] Von Arx J, Ziaie B, Dokmeci M and Najafi K 1995 Hermeticity testing of glass–silicon packages with on-chip feedthroughs *Transducers 95, Eurosensors* vol IX, pp 244–7
[25] Kovacs G T 1998 *Micromachined Transducers Sourcebook* 1st edn (New York: McGraw-Hill)
[26] Yuan Z, Garcia A L, Lopez G P and Petsev D N 2007 Electrokinetic transport and separations in fluidic nanochannels, review *Electrophoresis* **28** 595–610
[27] Honschoten J W v, Escalante M, Tas N R, Jansen H V and Elwenspoek M 2007 Elastocapillary filling of deformable nanochannels *J. Appl. Phys.* **101** 094310